Title
Direct Observation of Lipid Domains in Free-Standing Bilayers Using Two-Photon Excitation Fluorescence Microscopy

Journal
Journal of Fluorescence, 11(3)

ISSN
1053-0509

Authors
Bagatolli, Luis A
Gratton, Enrico

Publication Date
2001-09-01

DOI
10.1023/a:1012228631693

Journal of Fluorescence, Vol. 11, No. 3, September 2001 (© 2001)

Direct Observation of Lipid Domains in Free-Standing Bilayers Using Two-Photon Excitation Fluorescence Microscopy

Luis A. Bagatolli[1,3] and Enrico Gratton[2]

The direct observation of temperature-dependent lipid phase equilibria, using two-photon excitation fluorescence microscopy on giant unilamellar vesicles (GUVs) composed of different lipid mixtures, provides novel information about the physical characteristics of lipid domain coexistence. Physical characteristics such as the shape, size, and time evolution of different lipid domains are not directly accessible from the traditional experimental approaches that employ either small and large unilamellar vesicles or multilamellar vesicles. In this review article, we address the most relevant findings reported from our laboratory regarding the direct observation of lipid domain coexistence at the level of single vesicles in artificial and natural lipid mixtures. In addition, key points concerning our experimental approach will be discussed. The unique advantages of the fluorescent probe 6-dodecanoyl-2-dimethylaminonaphthalene (LAURDAN) under two-photon excitation fluorescence microscopy is particularly addressed, especially, the possibility of obtaining information on the phase state of different lipid domains directly from the fluorescent images.

KEY WORDS: Lipid domains; two-photon excitation fluorescence microscopy; giant unilamellar vesicles; free-standing bilayers.

INTRODUCTION

Studies of the physicochemical properties of artificial lipid systems, wherein the chemical and physical properties (such as lipid composition, pH, temperature, and pressure) can be systematically varied, provide important information about the behavior of the lipid matrix. In particular, a detailed understanding of phase equilibria in two- and three-component lipid bilayers constitutes a necessary step in the description of multicomponent lipid systems such as biological membranes. To this end, the effect of temperature on phase equilibria in lipid mixtures has been studied for almost 30 years and phase diagrams have been constructed using both theoretical and experimental approaches, in the latter case using mainly MLVs,[4] SUVs, or LUVs [1–13]. Important thermodynamic information is thus currently available for several lipid mixtures.

[1] Departamento de Química Biológica, Facultad de Ciencias Químicas, UNC, Pabellón Argentina, Ciudad Universitaria, 5000, Córdoba, Argentina.

[2] Laboratory for Fluorescence Dynamics, University of Illinois at Urbana–Champaign, Urbana, Illinois 61801.

[3] To whom correspondence should be addressed. Fax: +54 351 4334074. E-mail: lbagatol@dqb.fcq.unc.edu.ar

[4] *Abbreviations used:* LAURDAN, 6-dodecanoyl-2-dimethylaminonaphthalene; PRODAN, 6-propionyl-2-dimethylaminonaphthalene; *N*-Rh-DPPE, rhodamine B–1,2-dihexadecanoyl-*sn*-glycero-3-phosphoethanolamine (Lissamine); DOPC, 1,2-dioleoyl-*sn*-glycero-3-phosphocholine; POPC, 1-palmitoyl, 2-oleoyl-*sn*-glycero-3-phosphocholine; DLPC, 1,2-dilauroyl-*sn*-glycero-3-phosphocholine; DTPC, 1,2-ditridecanoyl-*sn*-glycero-3-phosphocholine; DMPC, 1,2-dimiristoyl-*sn*-glycero-3-phosphocholine; DPPC, 1,2-dipalmitoyl-*sn*-glycero-3-phosphocholine; DSPC, 1,2-distearoyl-*sn*-glycero-3-phosphocholine; DAPC, 1,2-diarachidoyl-*sn*-glycero-3-phosphocholine; DMPE, 1,2-dimiristoyl-*sn*-glycero-3-phosphoethanolamine; DPPE, 1,2-dipalmitoyl-*sn*-glycero-3-phosphoethanolamine; GSLs, glycosphingolipids; G_{M1}, Galβ1 → 3Gal-Nacβ1 → 4Gal(3 ← 2αNeuAc)β1 → 4Glcβ1 → 1′Cer; sphingomyelin, brain sphingomyelin; GUVs, giant unilamellar vesicles; LUVs, large unilamellar vesicles; MLVs, multilamellar vesicles; SUVs, small unilamellar vesicles.

1053-0509/01/0900-0141$19.50/0

A very interesting temperature regime in the lipid mixtures' phase diagram is that corresponding to the coexistence of different lipid phases. During the past few decades, the direct visualization of lipid domains in vesicles at the phase coexistence region was realized using electron microscopy techniques [14]. Even though the coexistence of different lipid phases is well established, no direct and detailed knowledge of the domains' shape and formation in bilayers was available [15]. Actually, there is a dearth of experimental approaches which allow direct visualization of the formation of lipid domains (shape and dynamics) in lipid bilayers using the same experimental conditions as in classical approaches (such as, for example, differential scanning calorimetry and fluorescence spectroscopy in cuvettes).

In this review article the reader will find two main sections, one devoted to the methodology and the other to a novel picture, at the level of single vesicles, of lipid phase coexistence in bilayers composed of natural and artificial lipid mixtures. Important information showing the physical characteristics of lipid domains in bilayers displaying gel/fluid and fluid ordered/fluid disordered phase coexistence is summarized. In addition, the unique advantages obtained from the combination of GUVs, three particular fluorescent probes (LAURDAN, PRODAN, and *N*-Rh-DPPE), and two-photon excitation fluorescent microscopy to follow lipid–lipid interactions at the level of single vesicles are discussed. In particular, the unique advantages of the LAURDAN probe to ascertain lipid domain coexistence using polarized excitation light are addressed in detail.

METHODOLOGY

As we mentioned above, our experimental approach combines the size of the GUVs (~30-μm mean diameter), the sectioning effect of the two-photon excitation microscope, and the fluorescent and partition properties of three particular fluorescent probes (LAURDAN, PRODAN, and N-Rh-DPPE). Compared with the traditional fluorescence studies involving lipid vesicles, this last combination offers a variety of unique advantages, such as (i) observation of different regions of a *single* vesicle using the sectioning capability of the two-photon excitation microscope; (ii) direct observation of the microscopic scenario in a single vesicle during the whole experiment without additional sample treatment (e.g., the specimen fixation process in the electron microscopy technique); (iii) the possibility of performing quantitative measurements; and (iv) direct correlation between the lipid domain morphology and the lipid domain phase state (using LAURDAN or PRODAN as the fluorescent probe).

In this section we address important aspects of our experimental approach, namely, GUVs, the fluorescent and partition properties of LAURDAN (more extensively), PRODAN, and *N*-Rh-DPPE, and two-photon excitation fluorescent microscopy.

GUVs

First, we want to emphasize that it is not our intention to revise deeply the giant vesicle field. However, we want to point out a few relevant details related to this interesting model system. GUVs are a very attractive system to study physical and biophysical aspects of lipid membranes using microscopy techniques, mainly because single vesicles can be easily observed under the microscope (GUVs have diameters of between 5 and 200 μm). The latter fact permits the possibility to observe directly the single-vesicle microscopic scenario, something that is not possible in experiments involving SUVs, LUVs, and MLVs. Another important aspect about GUVs is the fact that the size of these vesicles is of the same order as the size of cells, offering a proper model system to mimic the cell's plasma membrane.

An intense study of membrane physics has been done using GUVs, in particular, studies on the mechanical properties of model membranes [16–22]. These studies revealed the physical properties of the membranes through the calculation of elementary deformation parameters. GUVs offer an ideal artificial cell-size system to study aspects of lipid–lipid, lipid–protein, and lipid–DNA interactions. For that reason, giant vesicles have become an important tool in the membrane biophysical area in the last few years [23–33]. In this sense, an interesting review article was written by Menger and Keiper offering the reader an overview of the different studies using GUVs [22]. Likewise, an interesting book devoted completely to giant vesicles, edited by P. L. Luisi and P. Walde, appeared recently [34].

It is important to remark that different protocols were developed in many laboratories to prepare giant vesicles [35–39]. The latter fact can be explained since the mechanism of giant vesicle formation is still obscure. From our experience in giant vesicle formation we recommend the "electroformation method" developed by Angelova and Dimitrov [36,37]. The electroformation method provides a homogeneous population of GUVs, between 30 and 60 μm in diameter, in a short period of time (~1–2 h) with a high yield of unilamellar vesicles (~95%) [22,34,37]. The latter observation is remarkable since the yield of unilamellar vesicles obtained from other

methods is low (up to 20%), with a high incidence of multilamellar vesicles and other lipid structures such as lipid tubes. In this sense, a comparative analysis of the whole-sample characteristics obtained by the different methods was recently reported [40].

Fluorescent Probes

In this section the advantages of using particular fluorescent probes such as LAURDAN, PRODAN, and *N*-Rh-DPPE (Fig. 1) to ascertain lipid domain coexistence are summarized. The combination of the partition and fluorescent properties of these probes offers an excellent experimental tool to characterize the shape and phase state of lipid domains.

LAURDAN

The advantages of employing LAURDAN as a fluorescent probe to ascertain lipid domain coexistence using two-photon excitation fluorescence microscopy are unique. These advantages are based on three fundamental

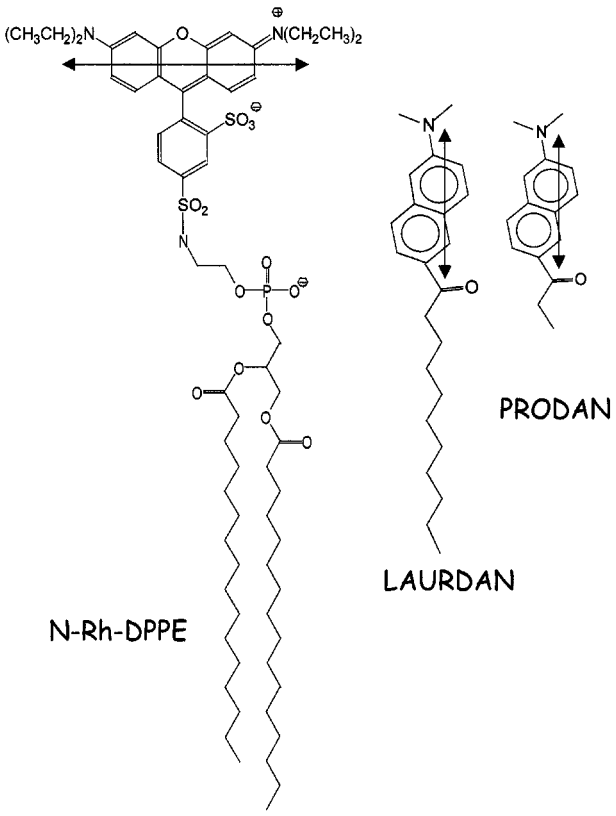

Fig. 1. Fluorescent molecules' molecular structure. The double arrow indicates the position of the excited dipole with respect to the plane of the lipid bilayer.

LAURDAN properties: (i) the electronic transition dipole of this molecule in lipid vesicles is aligned parallel to the hydrophobic lipid chains [29–31,41–43]; (ii) the phase-dependent emission spectral shift, i.e., LAURDAN's emission is blue in the ordered lipid phase and greenish in the disordered lipid phase [41–43]; and (iii) the homogeneous probe distribution on lipid membranes displaying phase coexistence [29–31,41,43].

Correlation of the LAURDAN Emission Spectral Shift with the Lipid Phase State. Several naphthalene derivatives belong to the family of polarity-sensitive fluorescent probes, first designed and synthesized by Gregorio Weber for the study of the phenomenon of dipolar relaxation of fluorophores in solvents, bound to proteins, and associated with lipids [44–46]. This family of probes includes LAURDAN and PRODAN. LAURDAN (and PRODAN) possesses large excited-state dipoles [44,45]. In polar solvents, and when the molecular dynamics of solvent dipoles occur on the time scale of the probe's fluorescence lifetime, a reorientation of solvent dipoles around the probe excited-state dipole may occur. The energy required for this reorientation results in continuous red shift of the fluorescence emission spectrum [41,43].

The origin of the dipolar relaxation observed in different lipids interfaces has been attributed to water molecules present in the bilayer at the level of the polar head group/hydrophobic chain region, where the LAURDAN fluorescent moiety resides [13,41,43,47–50]. The concentration and the molecular dynamics of water molecules change in the different lipid phase states. The latter effect is important when the lipid bilayer presents a loose lipid packing, i.e., the water reorientation with the probe's excited-state dipole occurs only in the fluid phase. The continuous red shift of the emission observed in the fluid phase, which increases upon raising the temperature, is due both to the increased concentration of water in the bilayer and to its increased dynamics. As a consequence, the gel and fluid lipid phases are characterized for blue (~440-nm) and green (490-nm) emission, respectively. Taking into account the homogeneous LAURDAN distribution in lipid membranes displaying phase coexistence [29–31,41,42], it is feasible to infer directly the phase state of a lipid domain in a GUV's fluorescent image using just a proper set of emission filters [30,31,33]. To our knowledge, the possibility of inferring the lipid phase state using fluorescent microscopy under these conditions (one probe with a homogeneous partition between the two coexisting phases) is a novel observation.

The LAURDAN Generalized Polarization Function. As we mention above, LAURDAN's emission spectrum is blue in the lipid gel phase, while in the liquid crystalline phase it moves, during the excited-state life-

time, from blue to green [41,43]. To quantify the emission spectral changes, the excitation generalized polarization (GP) function was defined analogously to the fluorescence polarization function as

$$GP = \frac{I_B - I_R}{I_B + I_R}$$

where I_B and I_R correspond to the intensities at the blue and red edges of the emission spectrum, respectively, using a given excitation wavelength [47,48]. It is important to remark that the GP measurement *does not imply the use of polarizers*. This well-characterized function is sensitive to the extent of water dipolar relaxation processes in the lipid bilayer, allowing the determination of the phase state of an unknown sample with the characteristic values obtained in pure gel or fluid phases (for reviews see Refs. 41–43).

The LAURDAN GP function on the GUV images is computed using two LAURDAN fluorescence images, one obtained in the blue (I_B) and other obtained in the green (I_R) regions of the LAURDAN emission spectrum. To obtain these LAURDAN fluorescence images for GP calculation, two optical band-pass filters, centered at 446 $\pm$ 23 nm (I_B) and at 499 $\pm$ 23 nm (I_R) (Ealing Electro-optics, New Englander Industrial Park, Holliston, MA), are used on the microscope [29–32,42].

The Effect of Photoselection to Ascertain the Lipid Domain's Phase State Using LAURDAN. The location of LAURDAN's excited-state dipole in the lipid membrane allows discrimination between ordered and disordered lipid domains as a result of the photoselection effect. The photoselection effect is dictated by the fact that only those fluorophores that are aligned parallel, or nearly so, to the plane of polarization of the excitation light become excited. Even though the use of polarized light on LAURDAN inserted in phospholipid membranes to ascertain the lipid domain phase state has been reported extensively in the literature [29–31,42], important aspects of this effect as a tool in our experimental system are carefully summarized in this section.

Domain Size Above the Resolution of the Microscope. Consider a circular polarization in the excitation light confined in the *x–y* plane. By exploring different regions of a spherical vesicle (at a given vertical section) we can observe that strong excitation occurs in the regions where LAURDAN's dipole is aligned parallel to the polarization plane of the excitation light (Fig. 2). Observing the *polar region* of a spherical lipid vesicle we find lower excitation compared with that obtained in the center region of the vesicle (Fig. 2) [29–31,42]. The latter difference is influenced by the phase state of the lipids. For example, observing a single-component lipid vesicle in the polar region, we obtain a dramatic difference in the fluorescent intensity values between the images of ordered and those of disordered lipid phases (Fig. 2). In an ordered lipid phase, such as the gel phase, the packing of the lipid molecules is very tight. The latter fact dramatically decreases the excitation of LAURDAN molecules in the polar region of the GUV because the position of the probe excited-state dipole is perpendicular to the polarization plane of the light. A different situation occurs in the polar region of GUVs displaying a disordered phase. In the latter case we always have a component of LAURDAN's transition dipole parallel to the excitation polarization because of the relatively low lipid order, i.e, the wobbling movement of LAURDAN molecule increases with respect to the gel phase (Fig. 2). This last fact allows more efficient LAURDAN excitation in the disordered lipid phase, i.e., a high emission intensity (see Fig. 2) [29–31,42].

When two lipid phases coexist in a single vesicle the photoselection effect on the LAURDAN molecule helps to ascertain the shape and infer the phase state of the coexisting lipid domains from images taken in the polar region of the GUVs (Fig. 3, top left) [29–31,42]. We want to point out that even though the LAURDAN fluorescent image in the top-left panel in Fig. 3 displays no fluorescence in the gel domain, the fluorescent probe is present in this domain (see Fig. 3, right). Certainly, the homogeneous distribution of LAURDAN molecules in bilayers composed of artificial mixtures displaying phase coexistence is one of the most interesting aspects of this fluorescent probe.

It is important to note that under conditions wherein the lipid domain's size is similar to or bigger than the image pixel size, the use of circular polarized excitation light offers an important advantage: the photoselection effect on LAURDAN operates only in the polar region of the vesicle (Figs. 2 and 3, bottom) [31]. In the equatorial region of the vesicle *all* LAURDAN molecules are excited without the influence of the photoselection effect because in this particular region the LAURDAN excited-state dipole is always parallel to the polarization plane of the excitation light (see Fig. 2). This last condition is necessary to obtain a uniform excitation over the entire fluorescent image, allowing proper calculation of the GP image (Fig. 3, top right). Measurements of the GP function in the polar region of the vesicle are inappropriate since the photoselection effect strongly influences the population of emitting LAURDAN molecules in the lipid membrane, giving an incomplete GP image.

To summarize, exciting LAURDAN with circular polarized light, under conditions where the size of lipid domains is similar to or bigger than the image pixel size,

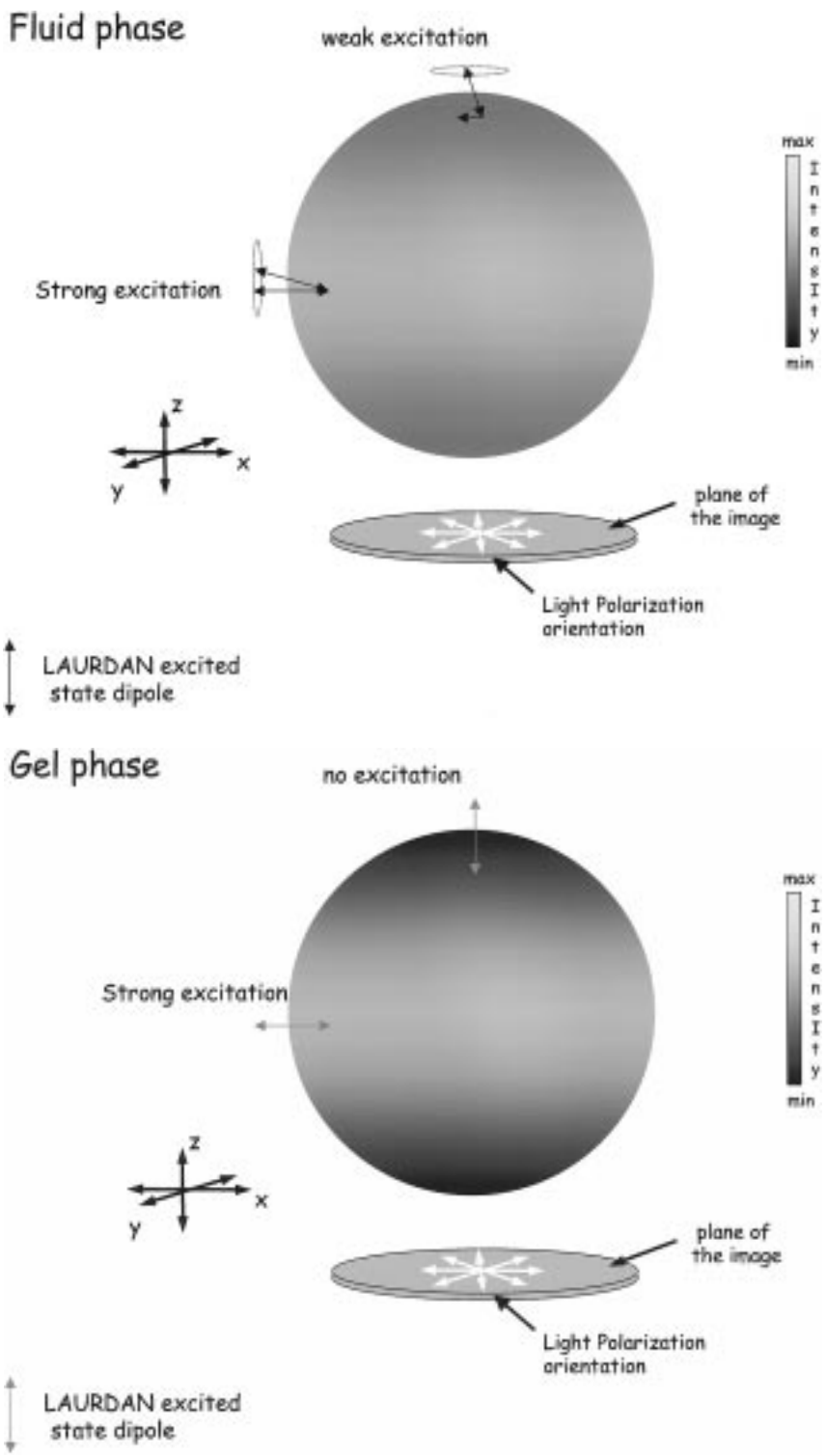

Fig. 2. Schematic representation of the photoselection effect using LAURDAN in single-component GUVs. Note that in the gel phase the efficiency of LAURDAN excitation is negligible with respect to that obtained in the fluid phase. The orientation and mobility restriction of the LAURDAN excited-state dipole in the gel phase with respect to the orientation of the circular polarized light explain this phenomenon (see text).

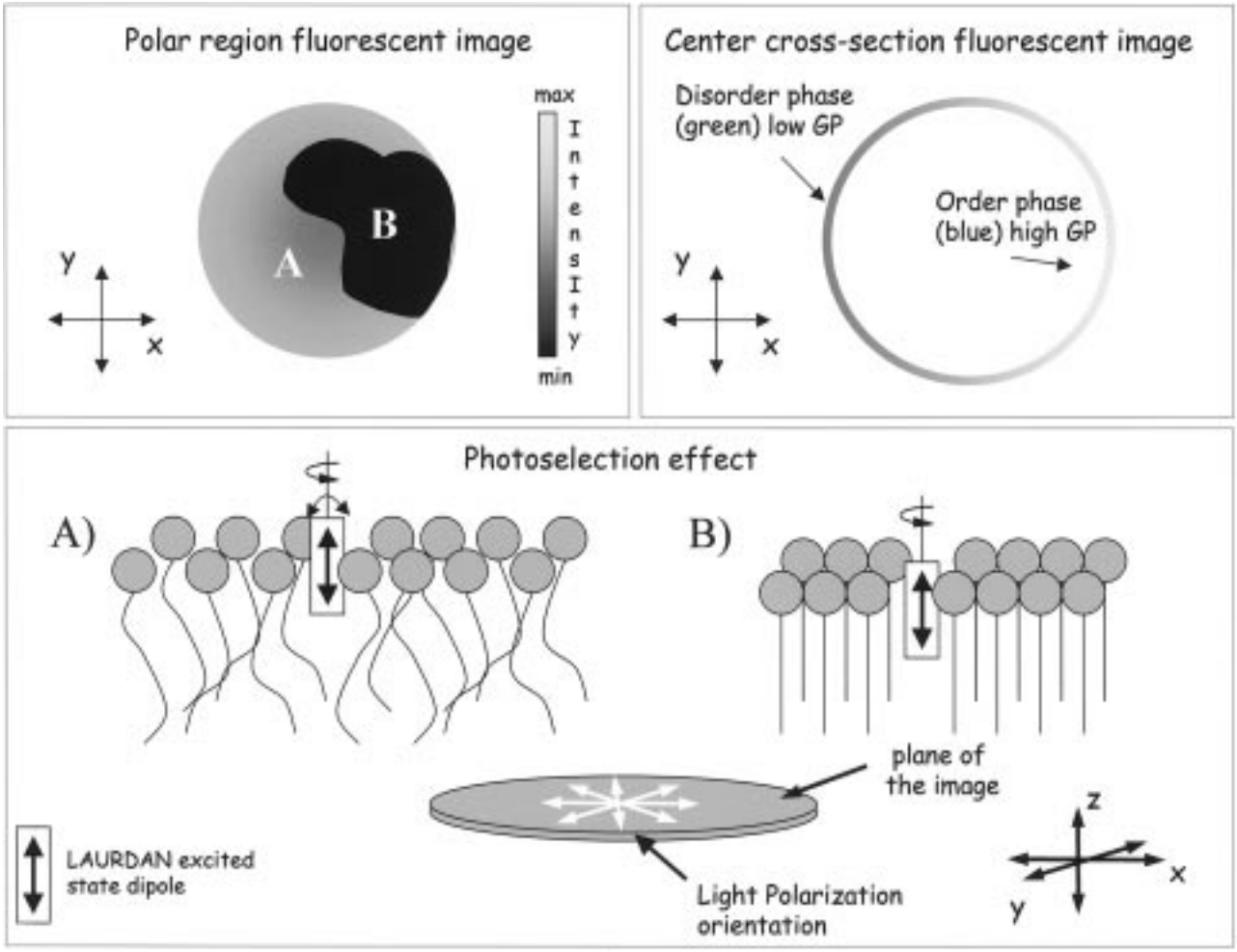

Fig. 3. Schematic representation of the photoselection effect (top left) and the phase-dependent fluorescent emission shift (top right) using circular polarized excitation light on LAURDAN-labeled GUV fluorescence intensity images in the phase coexistence temperature regime. The small double-headed curved arrows associated with the LAURDAN excited-state dipoles in the fluid phase (A) denote probe mobility (wobbling), which decreases dramatically in the gel phase (B).

allows one to extract information about (a) the orientation of the lipids in a particular domain (polar region, photoselection effect) and (b) the extent of the water dipolar relaxation process in the different lipid domains (equatorial region, GP) [31]. The latter information provides strong physical arguments to ascertain the phase state in lipid membranes.

Domain Size Below the Resolution of the Microscope. When the lipid domain's size is smaller than the image pixel size it is not possible to determine the lipid domain shape using the above-mentioned experimental approach. However, it is interesting to mention that it is possible to ascertain lipid domain coexistence obtaining LAURDAN GP images at the GUV's equatorial region with linear polarized light [29,30,42]. If the lipid domain size is smaller than the microscope resolution, each pixel of the image will present an average GP value. Since the polarized light, which photoselects appropriately oriented LAURDAN molecules, also selects LAURDAN molecules associated with high GP values, we can discriminate pixels with high and low GP values. Essentially, if the image contains separate domains (pixels) of different GP values because of lipid phase coexistence, the higher GP value domains appear parallel to the orientation of the polarized excitation light, and not in the perpendicular direction [29,30,42]. This effect was used to ascertain lipid domain coexistence in multilamellar vesicles composed of DLPC/DPPC mixtures [42] and GUVs composed of pure phospholipids [29].

PRODAN

Although PRODAN shows the same photoselection effect as LAURDAN (the excited state dipole is also

aligned perpendicular respect to the membrane plane, [30,51], this fluorescent molecule shows preferential partition to the fluid phase. The PRODAN partition coefficient is 35 times higher in the fluid phase with respect to the gel phase [52]. Compared to LAURDAN, PRODAN's solubility in water is high (LAURDAN's water solubility is negligible). Therefore the contribution of emission coming from the water is important in the case of PRODAN. Even though PRODAN's emission from water is easily subtracted in fluorescence cuvette experiments (PRODAN's water emission is red shifted with respect to that originating from lipid membranes [52]), the direct observation of the lipid membrane in the two-photon experiments elegantly circumvents this problem. PRODAN, as LAURDAN, also displays a lipid- phase-dependent spectral shift and the GP function in the lipid membrane can be easily computed from the GUV center cross-section images.

N-*Rh-DPPE*

A different situation was found using *N*-Rh-DPPE. This probe does not display any phase-dependent emission spectral shift. In addition, *N*-Rh-DPPE does not display the photoselection effect as does PRODAN or LAURDAN because the excited-state dipole of this probe is aligned parallel to the surface of the GUVs [30,31]. Using circularly polarized light, and as a consequence of the location of the *N*-Rh-DPPE excited-state dipole in the membrane, the fluorescence intensity at the top or center regions of a single-lipid component GUV is not affected by the lipid phase state as we reported for LAURDAN and PRODAN [30,31]. *N*-Rh-DPPE discriminates between gel and fluid lipid domains because the probe concentration changes dramatically between the coexisting lipid phases. In addition, the *N*-Rh-DPPE effective concentration in the gel and fluid lipid domains depends on the nature of the lipid binary mixture [30,31]. For example, in the phase coexistence temperature regime we found that *N*-Rh-DPPE is completely segregated from the gel domains in DPPE/DPPC, DMPE/DMPC, DLPC/DSPC, DLPC/DAPC, or DMPC/DSPC mixtures, while in DLPC/DPPC mixtures this probe shows a high affinity for the more ordered lipid domains (see Fig. 7) [30,31]. This last finding clearly shows that it is difficult to establish directly from the GUV's fluorescent image the lipid domain phase state using *N*-Rh-DPPE and that it is not wise to generalize the fluorescent molecule's affinity for the different lipid phases without a careful probe characterization.

In Table I we summarize the most relevant properties of LAURDAN, PRODAN, and *N*-Rh-DPPE under polarized light excitation.

The Advantages of Using Two-Photon Excitation Microscopy

To acquire the fluorescent images we used a scanning two-photon fluorescence microscope whose design and performance were discussed elsewhere [29–31,53,54]. Two-photon excitation is a nonlinear process in which a fluorophore absorbs two photons simultaneously. Each photon provides half the energy required for excitation. The high photon densities required for two-photon absorption are achieved by focusing a high-peak power laser light source on a diffraction-limited spot through a high numerical aperture objective [54–56]. Therefore, in the areas above and below the focal plane, two-photon absorption does not occur, because of insufficient photon flux. This phenomenon allows for a sectioning effect without using emission pinholes as in confocal microscopy [54–56]. Another advantage of two-photon excitation is the low extent of photobleaching and photodamage above and below the focal plane. The latter two effects are important in our experiments. In particular, the photobleaching effect on LAURDAN and PRODAN-labeled GUVs under two-photon excitation is considerably reduced with respect to one-photon excitation, where both sides of the vesicle are excited (Parasassi and Gratton, unpublished observations).

The possibility to obtain fluorescent images from different regions of the vesicle is an important fact in our experimental approach [29–31,42]. Therefore, it is important to mention that confocal microscopy can be equally used to obtain optical sections of the GUVs. In fact, the use of confocal microscopy (one-photon excitation) to ascertain phase coexistence with particular fluorescent probes (Dil-C_{20} and Bodipy-PC) at a constant temperature was reported using GUVs composed of phospholipid-containing ternary mixtures [27]. In that work, the phase state of lipid domains was determined by measuring the diffusion constant of the different fluorescent probes in the different lipid domains using fluorescence correlation spectroscopy [27]. Instead of discussing the general advantages and disadvantages of using confocal or multiphoton fluorescence microscopy, which are extensively revised in the literature (see Ref. 56), we prefer to compare some aspects of our experimental approach with the one reported by Korlach *et al.* [27] to study phase coexistence in GUVs. Although the information extracted from the GUV system about domain shape and phase state is similar using both experimental approaches, the use of LAURDAN offers a unique advantage: namely, the use of one probe (LAURDAN) provides simultaneous information on lipid domain shape and phase state from a simple fluorescent image.

Table I. Probe Characteristics in Artificial Lipid Mixtures

	LAURDAN	PRODAN	*N*-Rh-DPPE
Preferential partition between ordered and disordered lipid phases	No	Yes (fluid phase)	Yes (variable; depends on lipid composition)
Lipid phase-dependent emission spectral shift	Yes	Yes	No
Excited-state dipole orientation (with respect to the membrane plane)	Perpendicular	Perpendicular	Parallel

RESULTS AND DISCUSSION

Our experimental approach was applied to study several lipid samples, such as pure lipid components, binary phospholipid mixtures, phospholipid/cholesterol/sphingomyelin mixtures with and without the ganglioside G_{M1}, and some natural lipid extracts. The main intention of this section is to recapitulate the most relevant findings about the direct observation of lipid phase coexistence at the level of single vesicles. The results we summarize in this section were reported previously from our laboratory [29–33].

Samples That Display Gel/Fluid Phase Coexistence

GUVs Composed of Pure Phospholipids

Even though the thermotropic behavior of pure phospholipid components was studied extensively for many years using an array of techniques, our experimental approach allowed us for the first time to correlate simultaneously changes in vesicle morphology and lipid lateral organization at the level of single vesicles [29].

An interesting behavior concerning the vesicle morphology and phospholipid phase state was observed in GUVs composed of DTPC, DMPC, and DPPC at the corresponding phase transition temperature during cooling and heating cycles [29]. The vesicle diameters overshoot at the phase transition during the cooling cycle, displaying disjoint regions in LAURDAN GP images using linear polarized excitation light [29]. LAURDAN GP images at temperatures corresponding to the phase transition suggest the coexistence of gel and fluid domains of a size smaller than the microscope's resolution (0.3 μm) [29]. After the phase transition the vesicle's diameter decreased about 7–8% with a small drop in temperature corresponding to the lipid pretransition (observed in DMPC and DPPC GUVs) in LAURDAN GP images consisting of a pure gel phase [29]. The change in diameter corresponds to a decrease in the area of about 13–15%, similar to those reported by Needham and Evans in DMPC GUVs using the microaspiration test applying a moderate stress level on the lipid membrane [18]. Interestingly, during the heating cycle and in the main phase transition temperature's range, the vesicles display a sequence of different shapes as the temperature is increased as follows: spherical–polygonal–ellipsoidal (Fig. 4). Following the LAURDAN intensity with the blue band-pass filter (which selects preferentially the intensity coming from the phospholipid gel phase), we observed that the intensity coming from the flat parts was higher than that coming from the corners (see Fig. 4). This finding demonstrated that the flat parts correspond to gel phase regions, whereas the corners correspond to fluid regions. It is important to remark that even though we observed different events related to the vesicle morphology between the heating and the cooling cycles, no hysteresis in the main phase transition temperature value was observed [29].

To evaluate if the GUV's morphology related phenomena observed at the phase transition temperature are related to the lipid phase changes, experiments with the addition of cholesterol were performed [29]. The phenomena observed during the cooling and heating cycles are abolished in the presence of 30% cholesterol because of the absence of gel and fluid domains due to the well-known homogenizing effect of cholesterol. This last experiment confirms that the physical constraints imposed for the gel/fluid phase coexistence on the GUV's structure are responsible for its morphological changes during the heating and cooling cycles (polygonal shape and diameter change, respectively) at the main phase transition temperature [29].

A major question still remains as to the physical mechanism responsible for the formation of the polygonal vesicle shape at the transition temperature. We pointed out some possible contributions to this process [29]. (i) During the heating cycle, the gel phase regions are stressed by the curvature imposed by the spherical shape of the vesicles. When there is enough fluid phase, some parts of the vesicle still in the gel phase can assume a planar geometry to release tension due to the curvature.

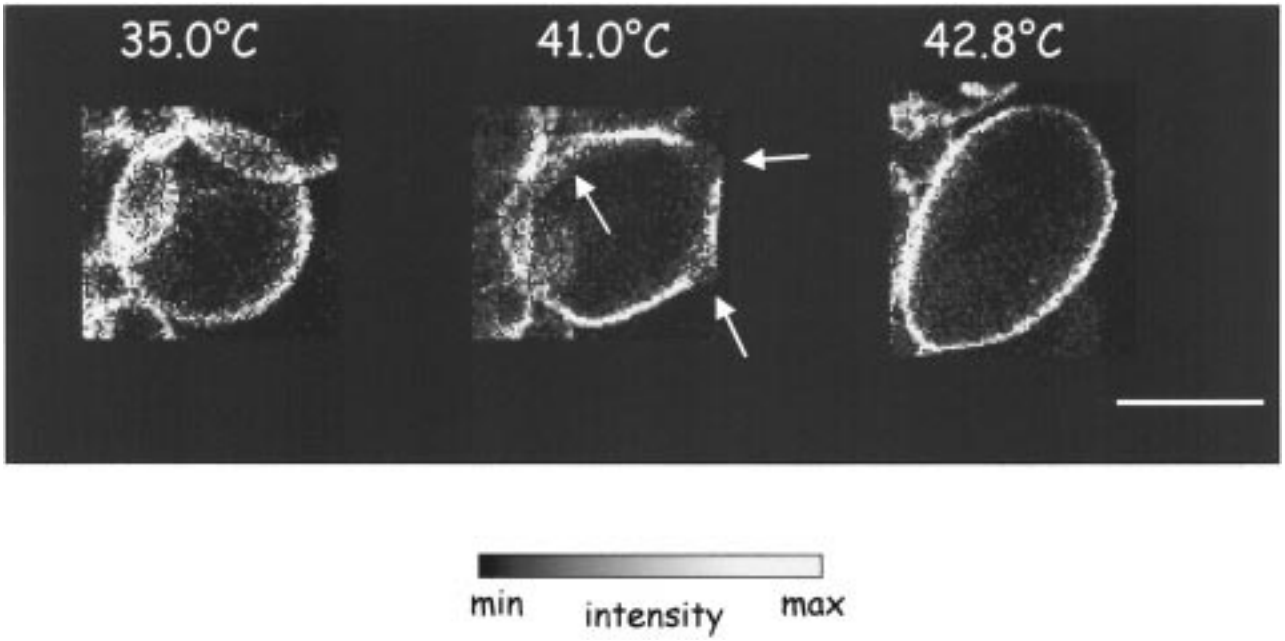

Fig. 4. Shape changes of a DPPC vesicle on passing through the main phase transition during the heating cycle. The images show the LAURDAN intensity in false color representation. The bar corresponds to 20 μm. The arrows show the low-intensity (fluid) regions. Adapted from Ref. 29.

Instead, the curvature is taken by the fraction of fluid regions, which are confined along the polygonal lines. (ii) During the heating cycle, water must penetrate into the vesicle to accommodate the larger diameter corresponding to the fluid phase. However, unless a pore is formed, the vesicle cannot expand. To accommodate the larger surface area with the same volume the vesicle must change shape, for example, assuming a polygonal shape. When a large enough pore is produced, the vesicle can relax to the spherical shape. (iii) The process described in ii is different during the cooling cycle. Now water must leave the vesicle interior to accommodate the smaller vesicle diameter corresponding to the gel phase. Only a spherically shaped vesicle can achieve the latter condition. When a pore is formed, water can exit the vesicle. This sudden flow may account for the shaking of the vesicle, which occurs at this temperature. In summary, the vesicle will attain whatever geometric shape is consistent with two constraints: (1) a given bilayer area and (2) a given interior volume, which is determined by the trapped water and the leakage rate across the membrane [29].

GUVs Composed of Binary Phospholipid Mixtures

The fluorescent images obtained from GUVs composed of phospholipid binary mixtures open a fascinating window through which important features about the lipid lateral organization can be extracted. In this section, we intend to present some particular trends obtained from the direct observation of several lipid mixtures, i.e., DLPC/DPPC, DLPC/DSPC, DLPC/DAPC, DMPC/DSPC, POPC/DPPC, DPPE/DPPC, and DMPE/DMPC [30,31]. These trends are related to some physical characteristics of the lipid domains such as shape and size and their correlation with some intrinsic properties of the lipid mixtures such as the lipid miscibility.

The Microscopic Scenario of Lipid Phase Coexistence. Examples of the temperature dependence of single GUVs composed of binary phospholipid mixtures (DPPE/DPPC and DLPC/DSPC) are shown in Fig. 5. This figure shows that *micron-size* gel (dark areas) lipid domains expanded and migrated around the vesicle surface as we decreased the temperature. Moreover, the migration of the gel domains dramatically decreased at temperatures close to the gel/fluid → gel phase transition (see Fig. 5B). The latter phenomena are independent of the nature of the lipid binary mixtures in all systems studied [30,31]. It is important to remark that the phase transition temperature values, i.e., fluid → gel/fluid and gel/fluid → gel, obtained in our experiments are in good agreement with those reported from the binary lipid mixture's phase diagrams [30,31].

Changes in the Molar Fraction of a Particular Lipid Binary Mixture at a Constant Temperature. Previous data suggested that the topology of the gel lipid domains varies

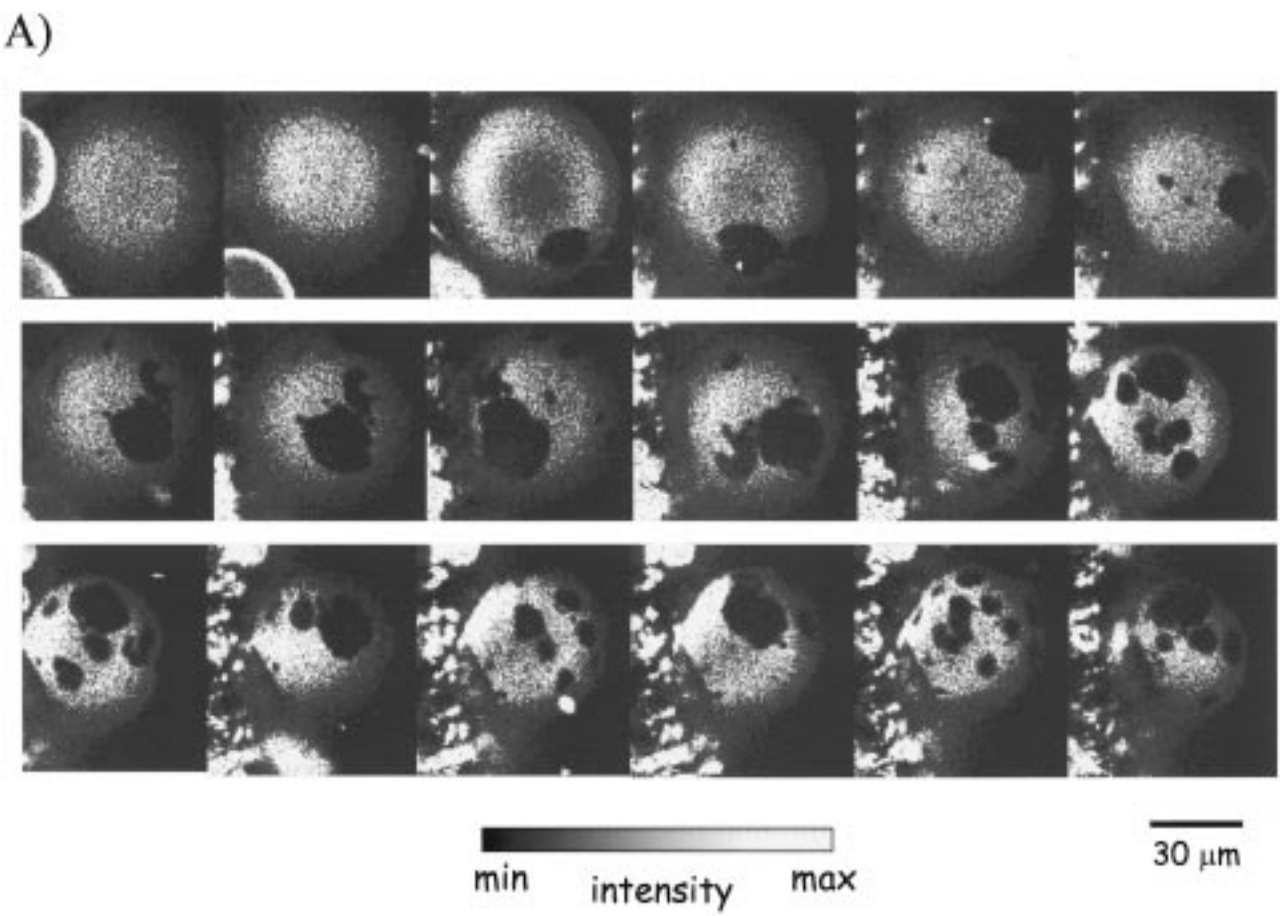

Fig. 5. Two-photon excitation fluorescence intensity images of *N*-Rh-DPPE-labeled GUVs composed of DLPC/DSPC, 1:1 mol (A), and DPPE/DPPC, 7:3 mol/mol (B), as a function of temperature (false color representation). The images were taken at the top part of the GUV. The temperature ramp was 55 to 28°C for DLPC/DSPC and 65 to 41°C for DPPE/DPPC. The probe concentration was below 0.25 mol%. The white arrow in the images indicates the fluid-to-gel/fluid phase transition for the high-melting lipid component. Adapted from Refs. 30 and 31.

across the phase diagram favoring a model in which the fluid-to-gel phase transition proceeds by an increase in the surface area of a constant number of gel phase domains instead of an increase in the number of the domains [57–59]. In a previous study we observed that changes in the lipid molar fraction affect the shape of the gel lipid domains [30]. For example, as shown in Fig. 6, different topologies and sizes of gel domains were observed for GUVs composed of 7:3 versus 3:7 mol/mol DPPE/DPPC [30]. The latter phenomenon was also observed for DMPE/DMPC binary phospholipid mixtures (Bagatolli, unpublished observation). Furthermore, as shown in Fig. 5, growth of the gel phase domains proceeds by the growth of a constant number of domains, in agreement with the model suggested above [57–59]. In our studies this phenomenon is independent of the nature of the different phospholipid binary mixtures.

Correlation Between the Lipid Mixture's Miscibility and the Gel Phase Domain's Size and Shape. An important observation from Fig. 5 is that the shape of the gel phase lipid domain changes with the nature of the lipid mixture. This dependence is well confirmed by the fluorescent images presented in Fig. 7 and can be related to the miscibility between the components of the binary mixture [30,31]. Two interesting observations can be extracted from Fig. 7. First, similar gel phase domain shapes were found for DLPC/DAPC, DMPE/DMPC, and DPPE/DPPC mixtures (leaf-shaped, large domains). These lipid mixtures present a low miscibility as predicted from the lipid phase diagram. Second, important changes in the gel domain's shape and size among the DLPC-containing mixtures (from a line shape to a quasi-circular shape to, finally, a leaf shape) are observed as the hydrophobic mismatch in the binary mixture increases.

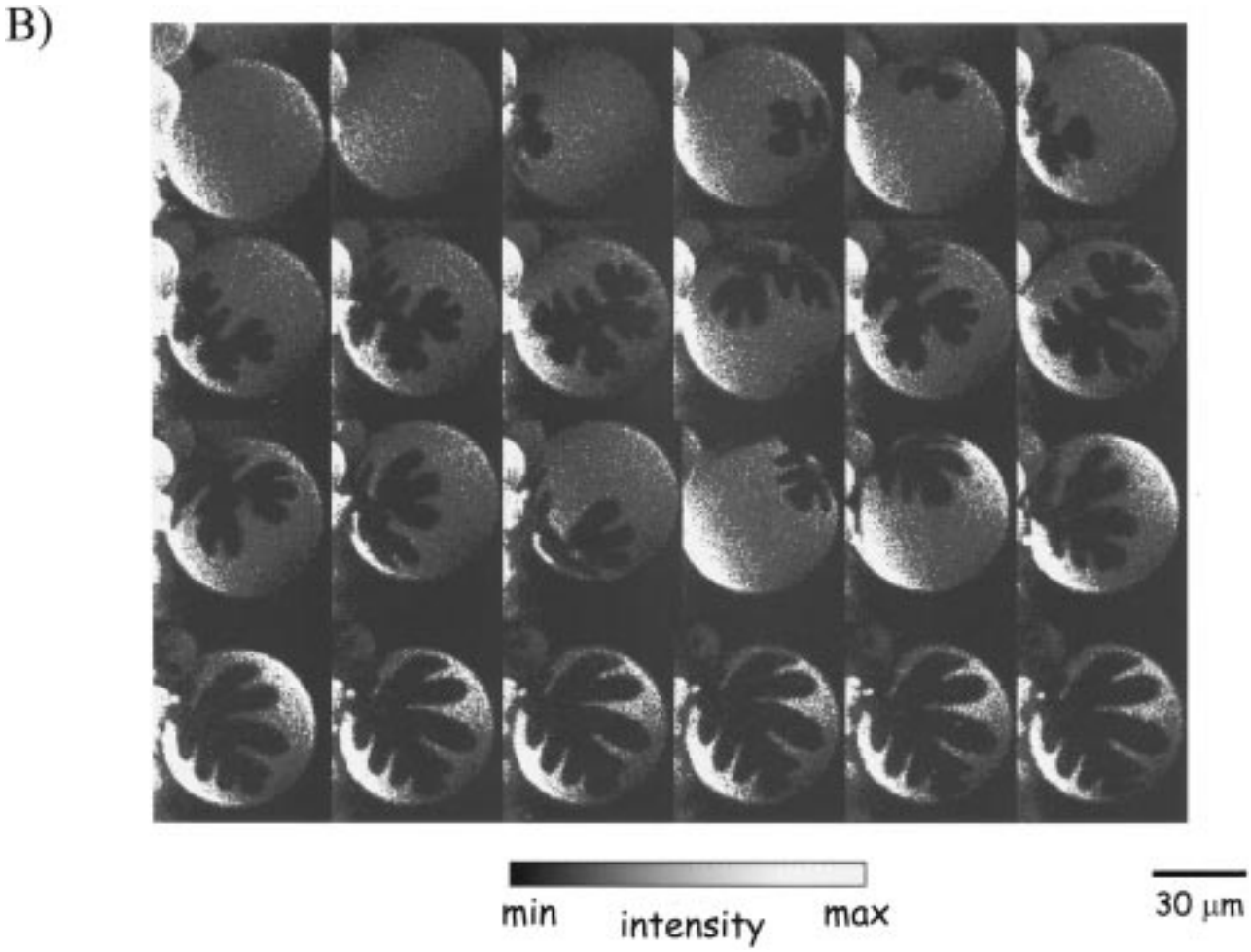

Fig. 5. Continued.

In this case the miscibility of the binary phospholipid mixture decreases as the hydrophobic mismatch in the binary mixture increases.

These observations are in agreement with considerations about the compositional and energetic differences between the gel and the fluid phase domain [59] and the incidence of the interfacial wetting effect [31,60]. In particular, the predicted large size of the gel lipid domains in low-miscibility lipid mixtures, because of the high compositional and high energetic differences between the coexisting gel and fluid domains [59,60], is confirmed by our images. Interestingly, the predicted ramified structure for a highly miscible lipid binary mixture [59–61] is observed in our images for DLPC/DPPC and DMPC/DSPC (see Fig. 7). In highly miscible phospholipid mixtures the compositional and energetic differences between the coexisting fluid and gel lipid phases are low and are expected to produce the formation of small gel phase domains and/or of a ramified structure in the lipid bilayer [59,61]. Although a ramified structure is observed in binary phospholipid mixtures that present a high miscibility and the average size of the gel domains is smaller than those observed for poorly miscible phospholipid binary mixtures (Fig. 7), micron-size gel domains are present in all the mixtures studied.

Interestingly, micron-size gel domains were observed in GUVs composed of phospholipid binary mixtures, in contrast with those observed in the phase coexistence temperature regime in GUVs composed of pure phospholipid, where the lipid domain size is below the microscope's resolution [29]. We speculate that the reason for the observed size difference of the gel domains should be related to an important compositional and energetic difference between the gel and the fluid domains in the latter two situations. It is reasonable to expect lower compositional and energetic differences between the

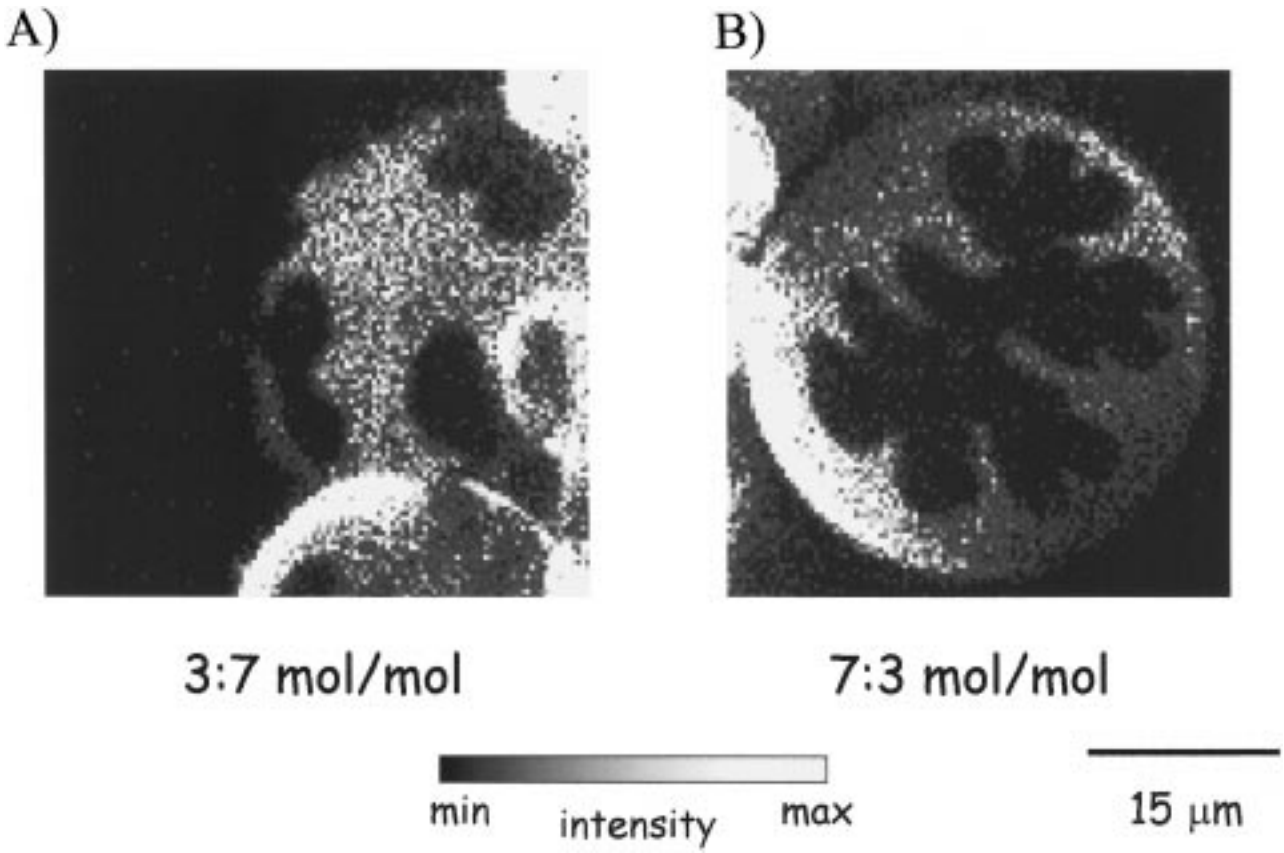

Fig. 6. Two-photon excitation fluorescence intensity images of *N*-Rh-DPPE-labeled GUVs composed of DPPE/DPPC, 3:7 mol (A) and 7:3 mol (B), 10° below the fluid-to-gel/fluid phase transition (false color representation). The images were taken at the top part of the GUV. Note the different shape of the gel fluid domains as the molar fraction of the DPPE changes (see text). The probe concentration was below 0.25 mol%. Adapted from Ref. 30.

coexisting phases for single-phospholipid GUVs since the same molecule is forming both phases.

Information of the Lipid Phase State Using the LAURDAN GP Function. As we mentioned under Methodology, it is possible to obtain information about the phase state of lipid domains using the LAURDAN GP function. For example, in a previous work we correlated the different lipid domain shapes observed in DLPC-containing binary mixtures (DLPC/DPPC, DLPC/DSPC, and DLPC/DAPC) with the phase state of the coexisting lipid domains [31]. Interestingly, a linear relationship between the LAURDAN GP values measured in the gel and fluid phase domains and the difference in the number of methylenes between the hydrophobic chains of DLPC and the second phospholipid component (ΔCH_2; Fig. 8) was obtained [31]. This finding supports the idea that the LAURDAN GP function is able to sense the compositional differences among the different gel phase lipid domains observed in the different lipid mixtures (see Fig. 8) [31]. In this sense, a linear dependence between the LAURDAN GP value and the intermolecular spacing among the lipid molecules in single-component aggregates formed of different glycosphingolipid (GSLs) and phospholipids was reported previously from our laboratory [49]. We explained this observation by considering the model introduced by Parasassi *et al.*, i.e., that LAURDAN in the lipid aggregates resides in sites containing different amounts of water and the dimensions of these sites are related to the lipid molecular structure and lipid packing characteristics [42]. Our results confirm the model proposed in our previous work [49], demonstrating the exquisite sensitivity of the GP function to the lipid lateral organization.

Lipid Domains: Micron Size or Nanometer Size? An interesting point to discuss here concerns the size of the gel lipid domains for binary phospholipid mixtures. Micron-size gel domains in bilayers composed of binary phospholipid mixtures were not predicted by theoretical models, and based on experimental data the size of gel domains was assumed to be between 10 and 100 nm in

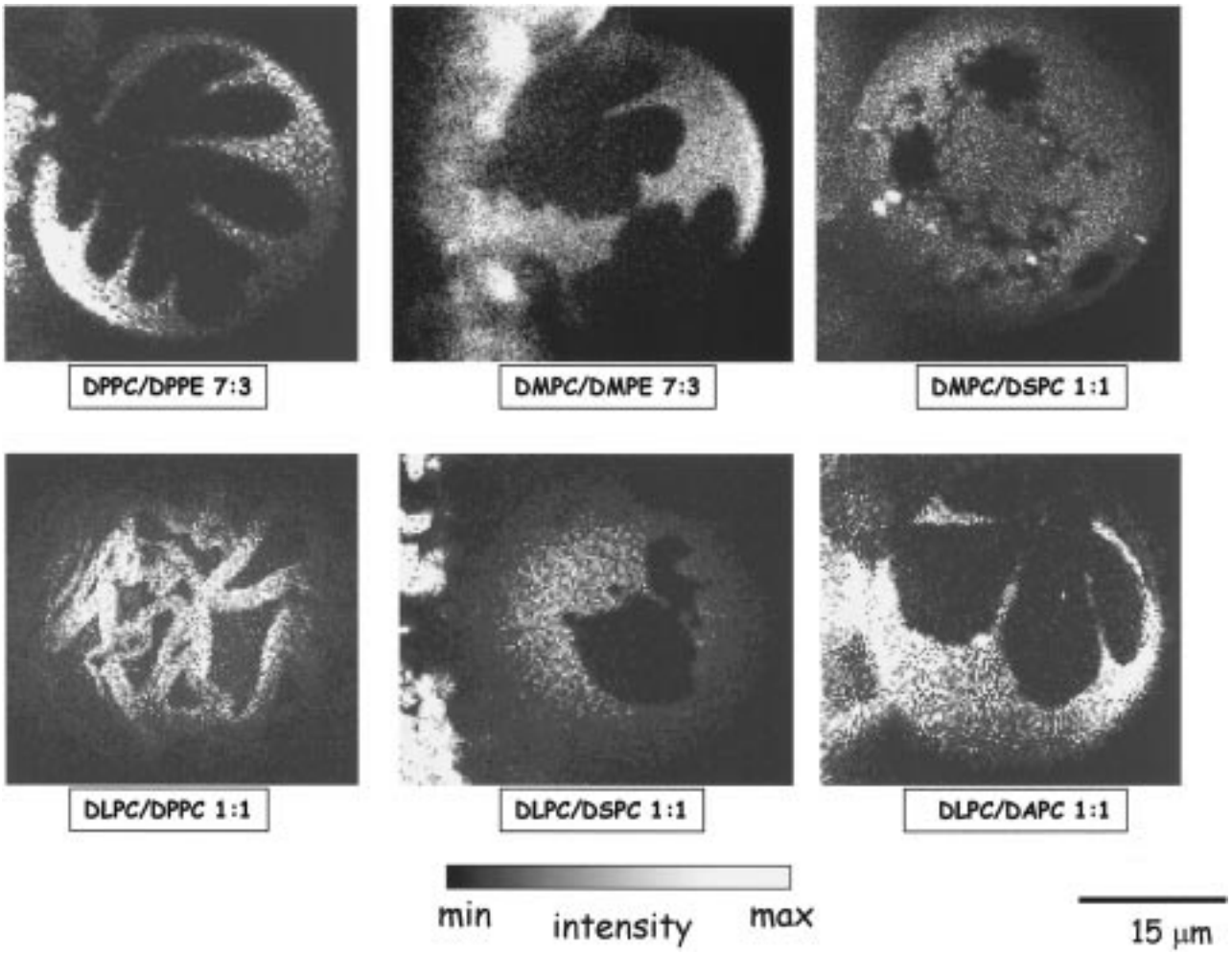

Fig. 7. Two-photon excitation fluorescence intensity images of *N*-Rh-DPPE-labeled GUVs composed of different binary mixtures at the fluid/gel phase transition temperature (false color representation). The images were taken at the top part of the GUV. Note that the partition of the probe in DLPC/DPPC is higher in the gel phase in contrast with the rest of the mixtures (see Methodology). The probe concentration was below 0.25 mol%. Adapted from Refs. 30 and 31.

diameter [14,42,59,60–62]. It is reasonable to think that the gel domain size obtained in SUVs and LUVs must be smaller than that found in GUVs because the different size among these lipid vesicles (100-nm diameter for SUVs, 400-nm diameter for LUVs and 300×10^2-nm diameter for GUVs). However, we want to remark that the ratio of the gel domain size to the vesicle size is quite similar among these different lipid vesicles (SUVs, LUVs, and GUVs). We do not find a plausible explanation for the gel phase domain size differences observed between our images (micron-size gel domains) in GUVs and those reported, for example, by Gliss *et al.* (gel domain average size, ~10 nm) in planar bilayers composed of a DMPC/DSPC mixture [31,62]. Both model systems (GUVs and planar membranes) present similar radii of curvature on the lipid molecular scale, and very reproducible domain sizes and shapes were observed between GUVs and planar lipid membranes with the same lipid mixture [33]. In this sense, it is important to note the similarities between the shape and size of the liquid condensed domains in monolayers and those of the gel domains found in GUVs composed of binary phospholipid mixtures [30,31]. In recent years a great variety of domain shapes in monolayer systems has been described in the literature (Refs. 63–65 and references therein). Theoretical models which consider the effect of long-range electrostatic interactions and line tension at the boundary of lipid domains on the shape of large, i.e., micron-size, lipid domains have been reported for lipid monolayers [15,65]. For lipid bilayers displaying lipid phase separation, Sackmann and Feder introduced a model that combines the theory of spinoidal decomposi-

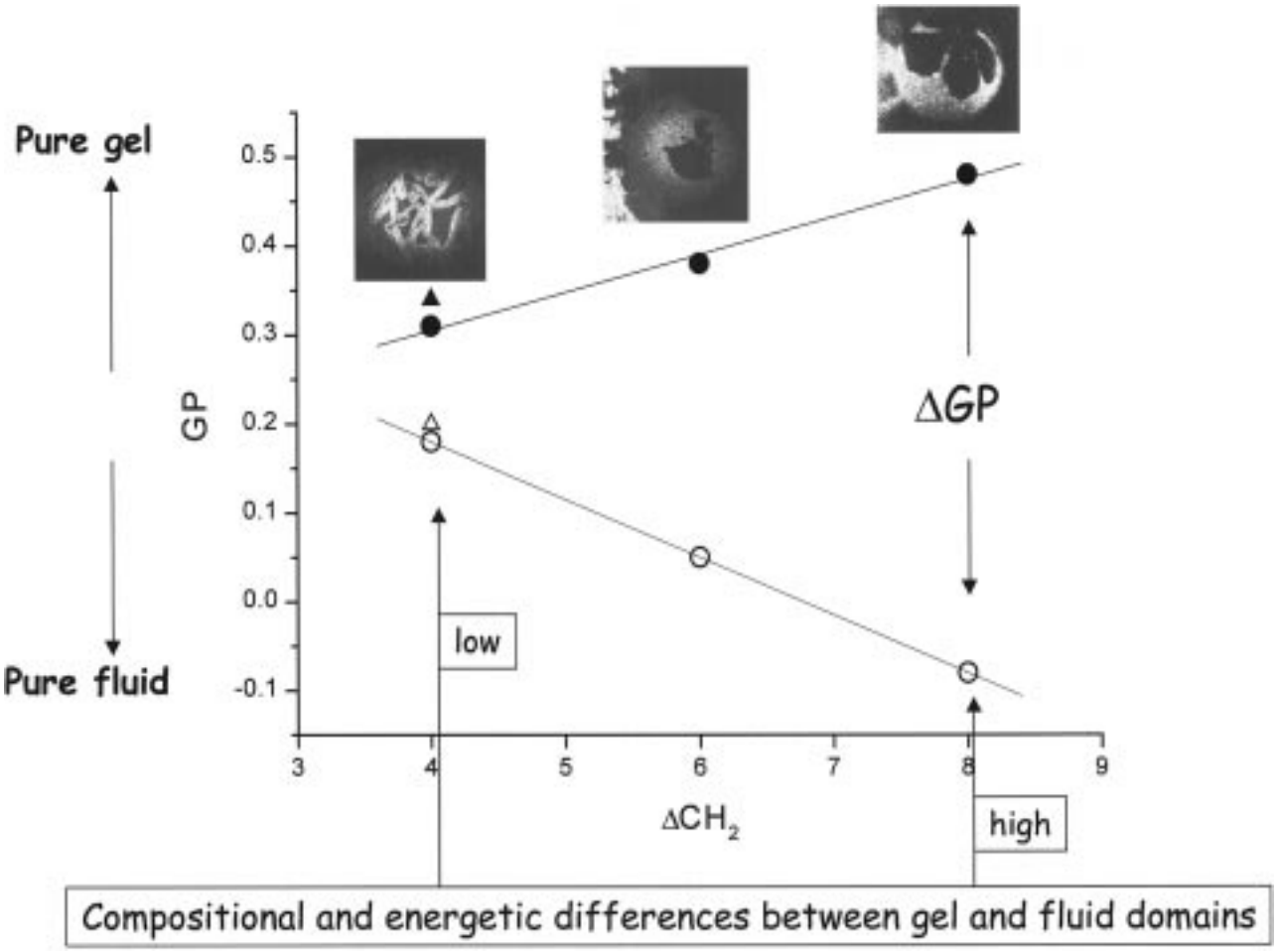

Fig. 8. LAURDAN GP vs the CH_2 difference between the hydrophobic chain lengths of the different PC binary mixtures. The open and filled symbols denote fluid and gel domains, respectively. (○, ●) DLPC-containing GUVs; (▲, △) DMPC/DSPC mixture. The ΔGP between the gel and the fluid components for DLPC/DAPC, DMPE/DMPC, and DPPE/DPPC was similar, showing a leaf shape. Adapted from Refs. 30 and 31.

tion and the membrane bending energy concept [66]. These authors show different domains shapes obtained by electron microscopy as stripe-like arrangements of two-dimensional precipitates and hexagonal arrangements of circular domains, both predicted by the theory. We observed a great variety of large domain shapes in free-standing bilayers composed of binary mixtures (several orders of magnitude larger than that reported from electron microscopy studies or from computer simulations). We believe that our experimental information will be useful for future theoretical models.

The Gel Phase Domains Span the Lipid Bilayer. One of the most important features of GUVs displaying gel/fluid phase coexistence fluorescence images concerns the symmetry of the gel domains along the normal of the bilayer surface (see Fig. 9 [30,31,67]). This finding is in agreement with the observations done in GUVs composed of mixtures of DLPC/DPPC/POPS at room temperature using confocal microscopy [27]. Independent of the lipid sample and the fluorescent probe, our images show a coupling between the inner and the outer leaflet of the bilayer [31]. Since these observations were done in different lipid mixtures, we conclude that the coupling between the inner and the outer leaflet of the bilayer in the phase coexistence temperature regime is a general phenomenon in samples that display gel–fluid phase coexistence. This phenomenon should be taken into account in theoretical models and computer simulations. As we pointed out in our previous work, it is possible that the molecular arrangement of the lipid molecules in the gel phase enhances the phospholipid tail–tail interaction [30,31]. These tail–tail interactions could drive the formation of a lipid cluster from one side of the bilayer plane to the other. This important observation, i.e., the fact that the

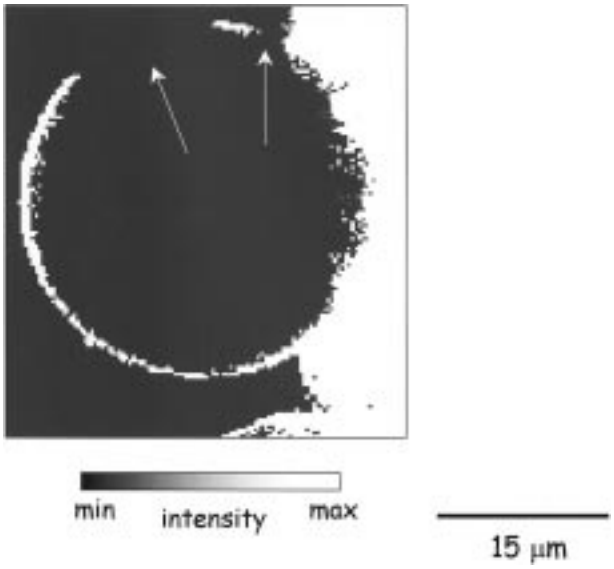

Fig. 9. Gel lipid domain spanning the lipid bilayer (white arrows). Two-photon excitation fluorescence intensity image of an *N*-Rh-DPPE-labeled GUV composed of DMPE/DMPC, 7:3 mol, in the phase gel/fluid phase coexistence's temperature regime (false color representation). The image was taken at the equatorial section of the GUV. The probe concentration was below 0.25 mol%.

gel domains span the lipid bilayer, confirms the existence of epitactic coupling in free-standing bilayers. Direct epitactic coupling has also been demonstrated in studies of supported membranes by Merkel *et al.* [68], where it was shown that gel domains in one monolayer induce solidification of domains of identical topology in a juxtaposed monolayer transferred from the fluid state.

Fluid Ordered/Fluid Disordered Phase Coexistence

The presence of cholesterol in phospholipid bilayers influences the physical characteristic of the membrane. In particular, the phase coexistence temperature region displays fluid ordered and fluid disordered lipid phases. This class of phase coexistence is postulated to exist in natural membranes and to have important biological roles. For example, the resistance of specialized lipid fractions and apically directed GPI-anchored proteins to extraction with cold nonionic detergent [69,70] in natural membrane preparations has led to the hypothesis of the existence of specialized glycosphingolipid microdomains termed "lipid rafts" [71]. The raft hypothesis proposes that certain naturally occurring lipids, such as sphingomyelin, phospholipid, glycosphingolipid, and cholesterol, differentially aggregate in the plane of the membrane driven solely by distinctive intermolecular interactions (van der Waals and hydrogen bonding interactions [71]). Liposomes formed from artificial raft lipid mixtures that mimic the composition of detergent—resistant membranes were partially resistant to detergent and showed spectroscopic evidence of ordered ("raft")/disordered phase coexistence [72,73]. In fact, domains with raft-like properties were found to coexist with fluid lipid regions both in planar supported lipid layers and in giant unilamellar vesicles (GUV) formed from (1) equimolar mixtures of phospholipid–cholesterol–sphingomyelin or (2) the natural lipids extracted from brush border membranes (BBM), which are rich in sphingomyelin and cholesterol [33]. Employing different fluorescent probes, rounded lipid domains, typically several microns in diameter, were observed by fluorescence microscopy (two-photon and epifluorescence) for artificial raft mixtures and BBM lipid extracts in planar supported lipid layers and GUVs, while nonraft mixtures (PC–cholesterol) appeared to be homogeneous [33]. Consistent with the raft hypothesis, G_{M1}, a glycosphingolipid, was highly enriched in the more ordered domains and resistant to detergent extraction, which disrupted the glycosphingolipid-depleted phase [33]. In GUVs formed from raft lipid mixtures or from BBM lipids, an array of more ordered and less ordered fluid domains that were in register in both monolayers could reversibly be formed and disrupted upon cooling and heating [33]. Besides offering novel direct details on the physical characteristics of fluid ordered/fluid disordered domain coexistence in artificial and natural lipid mixtures, the work of Dietrich *et al.* presents an interesting comparison between planar supported and free-standing bilayer model systems using the same lipid mixtures [33].

The Coexistence of Two Fluid Phases Is Discriminated Using LAURDAN. Let us consider now the occurrence of phase coexistence in GUVs composed of sphingomyelin/cholesterol/DOPC, 1:1:1 mol (Fig. 10). Using the LAURDAN molecule important information about coexisting lipid phases can be extracted from the experiments. The fluorescent images at the top region of the GUV, where the photoselection effect operates, display low and high micron-size fluorescent intensity areas, showing that LAURDAN is excited in both phases with different efficiencies (Fig. 10). This observation is in contrast with that found in mixtures that display gel/fluid phase coexistence, where no LAURDAN emission is observed from the gel phase domains [30,31]. This difference suggests that a fluid character is present in both lipid phases in GUVs composed of a sphingomyelin/cholesterol/DOPC mixture. One of the lipid phases is more ordered (low fluorescence intensity, strong photoselection effect) than the other. This fact is confirmed by using a band-pass filter that preferentially selects green

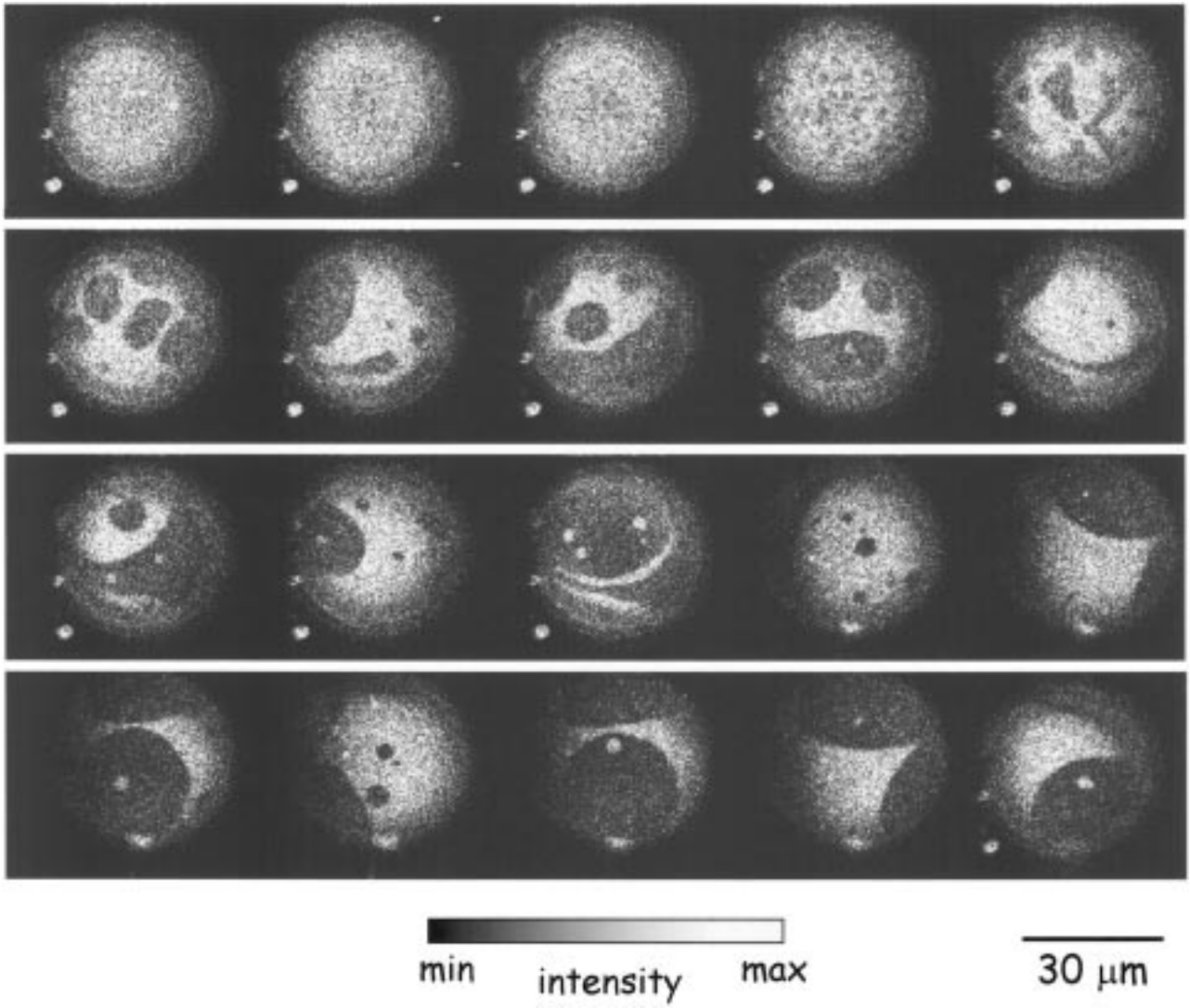

Fig. 10. Two-photon excitation fluorescence intensity images of LAURDAN-labeled GUVs composed of DOPC/sphyngomyelin/cholesterol, 1:1:1 mol, as a function of temperature (false color representation). The images were taken at the top part of the GUV. The temperature ramp was 33 to 25°C. Final LAURDAN/lipid ratio: 1:700, mol/mol.

emission intensity in the fluorescence image. Since LAURDAN fluorescence emission is greenish in the more disordered phase, the average intensity difference values between these two regions increases when the band-pass filter is used (not shown). This observation is confirmed at the center cross section of the vesicle by using the GP function. In the phase coexistence temperature region, well-defined regions (micron size) of different GP values are observed [33]. The GP difference between the coexisting domains is small, suggesting a strong influence between the coexisting lipid phases [30,31,33]. The perfectly round domains found in GUVs composed of a sphingomyelin/cholesterol/DOPC mixture (Fig. 10) indicate that both coexisting phases have a fluid character [33]. When fluid domains are embedded in a fluid environment, circular domains will form because both phases are isotropic and the line energy (tension), which is associated with the rim of two demixing phases, is minimized by optimizing the area-to-perimeter ratio. This picture contrasts with that found in the gel/fluid coexistence, where round domains are not observed [30,31]. Based on the LAURDAN information and the rounded shape of the lipid domains, we concluded that the phase coexistence in sphingomyelin/cholesterol/DOPC mixtures is between fluid ordered and fluid disordered lipid phases [33].

Natural Lipid Extracts Also Displays Fluid Ordered/Fluid Disordered Phase Coexistence. Although the lipid domains observed in brush border lipid extracts have rounded shapes (Fig. 11) as in the artificial raft mixture (sphingomyelin/cholesterol/DOPC), a very interesting phenomenon is that observed about the LAURDAN partition in the natural lipid mixture in the phase coexistence temperature regime. The LAURDAN concentration at the lipid membrane is homogeneous in all mixtures that present gel/fluid phase coexistence and in the artificial mixtures that display fluid ordered/fluid disordered phase coexistence (sphingomyelin/cholesterol/DOPC) [30,31,33]. In contrast with this trend, a lack of LAURDAN fluorescence from one of the coexisting phases is observed in BBMs (see inset in Fig. 11) [33]. This result implies either that the LAURDAN probe is excluded from the domains or that the fluorescence is nearly completely quenched in these domains [33]. This result demonstrates that in both scenarios the domains in these membranes made of natural lipids should be strongly selective for different lipids. This picture contrasts with that found in a cholesterol-free BBM (>95%) lipid extract, where the presence of irregularly shaped gel-like domains was observed and LAURDAN was present in both lipid phases [33]. The formation of the gel-like domains was observed at temperatures lower than those found for the cholesterol-containing BBM lipid extract, suggesting that a sphingomyelin-enriched gel-like phase occurs in the absence of cholesterol [33].

Fluid Ordered Lipid Domains Span the Lipid Bilayer. A very important fact is that the fluid ordered domains span the lipid membrane as was observed in samples displaying fluid/gel phase coexistence [30,31,33]. This phenomenon was found even in multicomponent lipid mixtures such as BBM lipid extracts (see Fig. 11, inset) [33] and basolateral membrane lipid extracts (Bagatolli and Levi, unpublished results), demonstrating that domains spanning the bilayer are not restricted to synthetic mixtures containing only a few lipid species but may exist in a natural multicomponent lipid mixture. This finding suggests that under certain conditions, raft domains in the outer monolayer of the plasma membrane have the potential to aggregate selected lipids in the inner monolayer [33]. This feature could

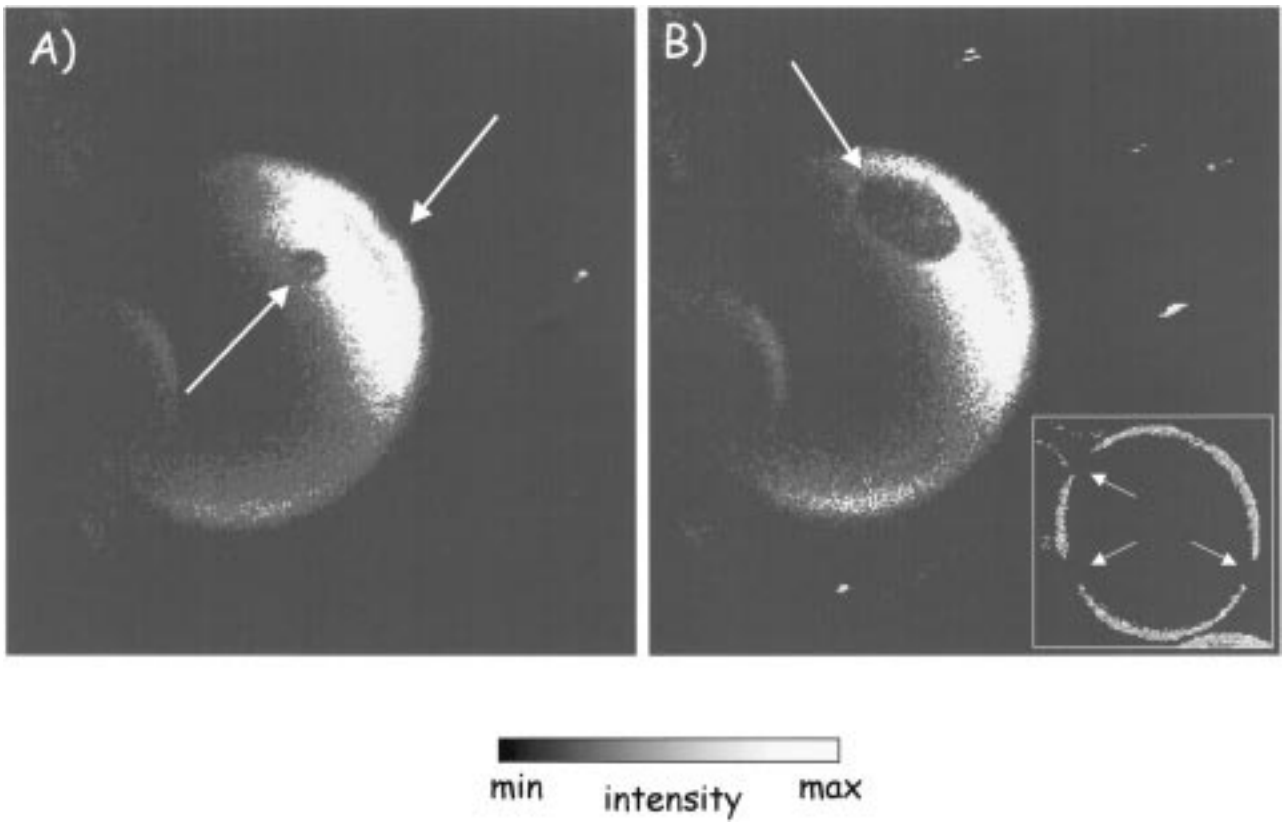

Fig. 11. Two-photon fluorescence images of polar sections (A, B) and equatorial sections (inset) of a LAURDAN-labeled GUV composed of extracted brush border membrane lipids: 30°C (A) and 25°C (B and inset; false color representation). The diameter of the vesicle was ~30 μm. Final LAURDAN/lipid ratio: 1:700, mol/mol. Adapted from Ref. 33.

provide a mechanism for how raft receptors in the outer monolayer are coupled to cytoplasmic components of signal transduction pathways—a question that has eluded simple answers [74]. Overall, the work of Dietrich *et al.* strongly supports the notion that in biomembranes selected lipids can aggregate laterally to form more ordered, detergent-resistant, lipid rafts into which glycosphingolipids partition [33].

Other Lipid Mixtures Displaying Phase Coexistence

We briefly describe the observations we did in the polar lipid fraction E (PLFE) from the thermoacidophilic archaebacteria *Sulfolobus acidocaldarius* using two-photon excitation microscopy [32]. The major component of the plasma membrane of *S. acidocaldarius* is bipolar tetraether lipid (~90% of the total lipids) and the polar lipid fraction E (PLFE) is the main constituent [75]. PLFE is composed of approximately 10% glycerol dialkylglycerol tetraether (GDGT), with phosphatidylmyoinositol attached to one glycerol and β-D-galactosyl-D-glucose to the other (Fig. 12A), and about 90% glycerol dialkylnonitol tetraether (GDNT), containing phosphatidylmyoinositol on one end and β-glucose on the other (Fig. 12B). Both GDGT and GDNT consist of a pair of 40-carbon phytanyl hydrocarbon chains. Each of the biphytanyl chains contains up to four cyclopentane rings, and the number of these rings increases with increasing growth temperature [76].

The first difference between giant vesicles composed of PLFE lipids and GUVs composed of phospholipid mixtures is that the PLFE membrane is a monolayer. Evaluating the insertion of a LAURDAN probe to PLFE interfaces, we found that the location of the LAURDAN dipole in these interfaces is parallel to the plane of the lipid surface, in contrast with that observed in phospholipid-containing GUVs [32]. When excited with light polarized in the *y*-direction, LAURDAN fluorescence in the center cross section of PLFE GUVs exhibits a photoselection effect, showing much higher intensities in the *x*-direction of the vesicles [32]. The *x*-direction photoselection effect and the low GP values obtained over a very large temperature range (10 to 70°C) lead us to propose further that the LAURDAN chromophore resides in the polar head-group region of PLFE liposomes, while the lauroyl tail inserts into the hydrocarbon core of the membrane. This unusual L-shape disposition is presumably caused by the unique lipid structures and by the rigid and tight membrane packing in PLFE liposomes [32]. In addition, the GP exhibited a small but abrupt decrease near 50°C, suggesting a conformational change in the polar head-groups of PLFE in agreement with the *d*-spacing data recently measured by small-angle X-ray diffraction and with the pyrene-labeled phosphatidylcholine and perylene fluorescence data previously obtained from PLFE multilamellar vesicles [32,77]. Interestingly, the two-photon LAURDAN fluorescence images showed snowflake-like lipid domains in PLFE GUVs at pH 7.23 and low temperatures (<20°C in the cooling scan and <24°C in the heating scan) as shown in Fig. 13. The location of the LAURDAN dipole and the fluorescence images taken at the giant vesicle equatorial region suggest

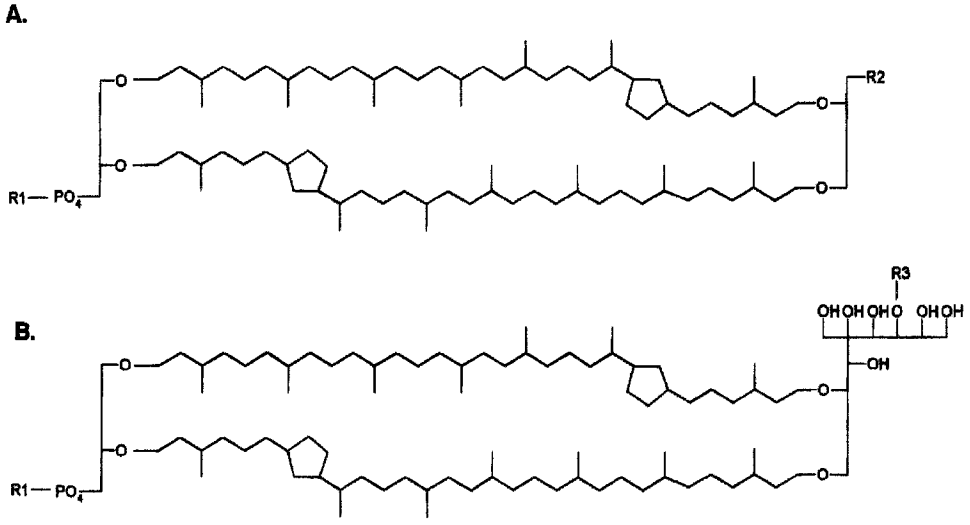

Fig. 12. Structures of PLFE lipids: (**A**) glycerol dialkylglycerol tetraether (GDGT) and (**B**) glycerol dialkylnonitol tetraether(GDNT). R1 = inositol; R2 = β-D-glucopyranose; R3 = β-D-galactosyl-β-D-glucopyranose. Adapted from Ref. 77.

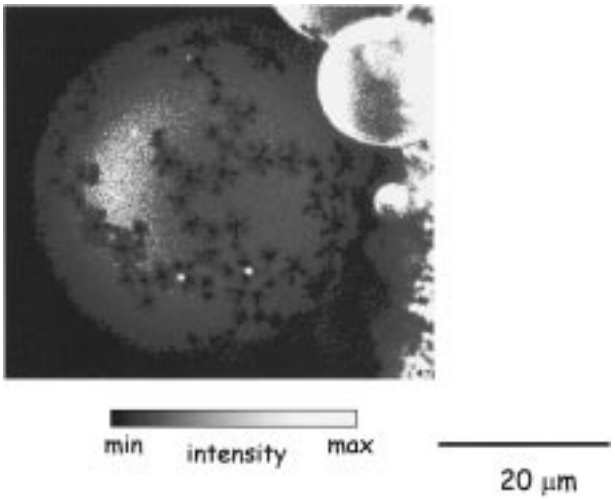

Fig. 13. Two-photon fluorescence image of a LAURDAN-labeled GUV composed of PLFE lipids at 15°C (false color representation). The image was taken at the polar region of the giant vesicle. Final LAURDAN/lipid ratio: 1:400, mol/mol. Adapted from Ref. 32.

probe segregation from the snowflake domains [32]. These domains, attributable to lipid lateral separation, were stable and laterally immobile at low temperatures (<23°C), suggesting tight membrane packing in the PLFE GUVs [32]. Although we believe that the snowflake domains are highly rigid, the shapes of these domains are very peculiar and different from those found in samples that display gel/fluid phase coexistence (compare Fig. 13 with Fig. 7). We believe that a particular compromise between compositional and energy differences between the two coexisting phases should explain the peculiar domain shape. Another important question is if the domain coexistence found in the model system has biological relevance for the living cell membrane. Further studies will be necessary to answer these questions.

CONCLUDING REMARKS

In this review article we have recapitulated the most relevant observations of lipid domain coexistence at the level of single vesicles reported recently from our laboratory, emphasizing particularly our new experimental approach. The novel information related to lipid domain formation, lipid domain shape and size, and their relationship with the nature of the lipid mixture opens up exciting new prospects for understanding the relevance of this phenomenon in more complex systems such as biological membranes. In this sense, the direct observation of phase coexistence with lipid domains spanning the lipid bilayer in natural lipid extracts of complex lipid composition is remarkable. This new information certainly opens new avenues of inquiry that may help us to understand the precise role of lipids in biological membranes, in particular, why cell membranes contain such an enormous assortment of different lipid species.

ACKNOWLEDGMENTS

This work was supported by grants from the NIH (RR03155) and Fundacion Antorchas. L.A.B. is a member of the CONICET (Argentina), Investigator Career.

REFERENCES

1. J. H. Ipsen and O. G. Mouritsen (1988) *Biochim. Biophys. Acta* **944**, 121–134.
2. K. Jørgensen and O. G. Mouritsen (1995) *Biophys. J.* **69**, 942–954.
3. A. G. Lee (1975) *Biochim. Biophys. Acta* **413**, 11–23.
4. B. R. Lentz, Y. Barenholtz, and T. E. Thompson (1976) *Biochemistry* **15**, 4529–4537.
5. S. Mabrey and J. M. Sturtevant (1976) *Proc. Natl. Acad. Sci. USA* **73**, 3862–3866.
6. P. W. M. Van Dijck, A. J. Kaper, H. A. J. Oonk, and J. De Gier (1977) *Biochim. Biophys. Acta* **470**, 58–69.
7. K. Arnold, A. Lösche, and K. Gawrisch (1981) *Biochim. Biophys. Acta* **645**, 143–148.
8. A. Blume, R. J. Wittebort, S. K. Das Gupta, and R. G. Griffin (1982) *Biochemistry* **21**, 6243–6253.
9. M. Caffrey and F. S. Hing (1987) *Biophys. J.* **51**, 37–46.
10. E. J. Shimshick and H. M. McConnell (1973) *Biochemistry* **12**, 2351–2360.
11. B. Maggio (1985) *Biochim. Biophys. Acta* **815**, 245–258.
12. B. Maggio, G. D. Fidelio, F. A. Cumar, and R. K. Yu (1986) *Chem. Phys. Lipids* **42**, 49–63.
13. L. Bagatolli, B. Maggio, F. Aguilar, C. P. Sotomayor, and G. D. Fidelio (1997) *Biochim. Biophys. Acta* **1325**, 80–90.
14. E. Sackmann (1978) *Ber. Bunsenges Phys. Chem.* **82**, 891–909.
15. A. Raudino (1995) *Adv. Coll. Interf. Sci.* **57**, 229–285.
16. E. Evans and R. Kwok (1982) *Biochemistry* **21**, 4874–4879.
17. D. Needham, T. M. McIntosh, and E. Evans (1988) *Biochemistry* **27**, 4668–4673.
18. D. Needham and E. Evans (1988) *Biochemistry* **27**, 8261–8269.
19. P. Meléard, C. Gerbeaud, T. Pott, L. Fernandez-Puente, I. Bivas, M. D. Mitov, J. Dufourcq, and P. Bothorel (1997) *Biophys. J.* **72**, 2616–2629.
20. P. Meléard, C. Gerbeaud, P. Bardusco, N. Jeandine, M. D. Mitov, and L. Fernandez-Puente (1998) *Biochimie* **80**, 401–413.
21. E. Sackmann (1994) *FEBS Lett.* **346**, 3–16.
22. F. M. Menger and J. S. Keiper (1998) *Curr. Opin. Chem. Biol.* **2**, 726–732.
23. R. Wick, M. I. Angelova, P. Walde, and P. Luisi (1996) *Chem. Biol.* **3**, 105–111.
24. M. L. Longo, A. J. Waring, L. M. Gordon, and D. A. Hammer (1998) *Langmuir* **14**, 2385–2395.
25. P. Bucher, A. Fischer, P. L. Luisi, T. Oberholzer, and P. Walde (1998) *Langmuir* **14**, 2712–2721.
26. M. I. Angelova, N. Hristova, and I. Tsoneva (1999) *Eur. Biophys. J.* **28**(2), 142–150.
27. J. Korlach, P. Schwille, W. W. Webb, and G. W. Feigenson (1999) *Proc. Natl. Acad. Sci. USA* **96**, 8461–8466.
28. J. M. Holopainen, M. I. Angelova, and P. K. J. Kinnunen (2000) *Biophys. J.* **78**(2), 830–838.

29. L. A. Bagatolli and E. Gratton (1999) *Biophys. J.* **77**, 2090–2101.
30. L. A. Bagatolli and E. Gratton (2000) *Biophys. J.* **78**(1), 290–305.
31. L. A. Bagatolli and E. Gratton (2000) *Biophys. J.* **79**, 434–447.
32. L. A. Bagatolli, E. Gratton, T. K. Khan, and P. L. G. Chong (2000) *Biophys. J.* **79**, 416–425.
33. C. Dietrich, L. A. Bagatolli, Z. Volovyk, N. L. Thompson, M. Levi, K. Jacobson, and E. Gratton (2001) *Biophys. J.* **80**, 1417–1428.
34. R. L. Luisi and P. Walde (Eds.) (2000) *Giant Vesicles*, ETH, Zürich, Switzerland.
35. J. P. Reeves and R. M. Dowben (1969) *J. Cell. Physiol.* **73**, 49–60.
36. M. I. Angelova and D. S. Dimitrov (1986) *Faraday Discuss. Chem. Soc.* **81**, 303–311.
37. M. I. Angelova, S. Soléau, Ph. Meléard, J. F. Faucon, and P. Bothorel (1992) *Progr. Colloid Polym. Sci.* **89**, 127–131.
38. A. Moscho, O. Orwar, D. T. Chiu, B. P. Modi, and R. N., Zare (1996) *Proc. Natl. Acad. Sci. USA* **93**, 11443–11447.
39. K. Akashi, H. Miyata, H. Itoh, and K. Kinosita Jr. (1996) *Biophys. J.* **71**, 3242–3250.
40. L. A. Bagatolli, T. Parasassi, and E. Gratton (2000) *Chem. Phys. Lipids* **105**(2), 135–147.
41. T. Parasassi and E. Gratton (1995) *J. Fluoresc.* **5**, 59–70.
42. T. Parasassi, E. Gratton, W. Yu, P. Wilson, and M. Levi (1997) *Biophys. J.* **72**, 2413–2429.
43. T. Parasassi, E. Krasnowska, L. A. Bagatolli, and E. Gratton (1998) *J. Fluoresc.* **8**, 365–373.
44. G. Weber and F. J. Farris (1979) *Biochemistry* **18**, 3075–3078.
45. R. B. Macgregor and G. Weber (1986) *Nature (Lond.)* **319**, 70–73.
46. T. Parasassi, F. Conti, and E. Gratton (1986) *Cell. Mol. Biol.* **32**, 103–108.
47. T. Parasassi, G. De Stasio, A. d'Ubaldo, and E. Gratton (1990) *Biophys. J.* **57**, 1179–1186.
48. T. Parasassi, G. De Stasio., G. Ravagnan, R. M. Rusch, and E. Gratton (1991) *Biophys. J.* **60**, 179–189.
49. L. A. Bagatolli, E. Gratton, and G. D. Fidelio (1998) *Biophys. J.* **75**, 331–341.
50. L. A. Bagatolli, T. Parasassi, G. D. Fidelio, and E. Gratton (1999) *Photochem. Photobiol.* **70**, 557–564.
51. E. K. Krasnowska, L. A. Bagatolli, E. Gratton, and T. Parasassi (2001) *Biochim. Biophys. Acta* **1511**, 330–340.
52. E. Krasnowska, E. Gratton, and T. Parasassi (1998) *Biophys. J.* **74**, 1984–1993.
53. P. T. C. So, T. French, W. M. Yu, K. M. Berland, C. Y. Dong, and E. Gratton (1995) *Bioimaging* **3**, 49–63.
54. P. T. C. So, T. French, W. M. Yu, K. M. Berland, C. Y. Dong, and E. Gratton (1996) in X. F. Wang and B. Herman (Eds.), *Chemical Analysis Series, Vol. 137*, John Wiley and Sons, New York, pp. 351–374.
55. W. Denk, J. H. Strickler, and W. W. Webb (1990) *Science* **248**, 73–76.
56. B. R. Master, P. T. C. So, and E. Gratton (1999) in *Fluorescent and Luminescent probes*, 2nd ed., Academic Press, New York, pp. 414–432.
57. M. B. Sankaram, D. Marsh, and T. E. Thompson (1992) *Biophys. J.* **63**, 340–349.
58. B. Piknova, D. Marsh, and T. E. Thompson (1996) *Biophys. J.* **71**, 892–897.
59. V. Schram, H. N. Lin, and T. E. Thompson (1996) *Biophys. J.* **71**, 1811–1822.
60. K. Jørgensen, M. M. Sperotto, O. G. Mouritsen, J. H. Ipsen, and M. J. Zuckermann (1993) *Biochim. Biophys. Acta* **1152**, 135–145.
61. T. Parasassi, G. Ravagnan, R. M. Rusch, and E. Gratton (1993) *Photochem. Photobiol.* **57**, 403–410.
62. C. Gliss, H. Clausen-Schaumann, R. Gunther, S. Odenbach, O. Randl, and T. M. Bayerl (1998) *Biophys. J.* **74**, 2443–2450.
63. R. M. Weis, and H. M. McConnell (1985) *J. Phys. Chem.* **89**, 4453–4459.
64. R. G. Oliveira, and B. Maggio (2000) *Neurochem. Res.* **25**, 77–86.
65. H. Möhwald, A. Dietrich, C. Böhm, G. Brezesindki, and M. Thoma (1995) *Mol. Membr. Biol.* **12**, 29–38.
66. E. Sackmann and T. Feder (1995) *Mol. Membr. Biol.* **12**, 21–28.
67. L. A. Bagatolli, T. Parasassi, G. D. Fidelio, and E. Gratton (1999) *Biophys. J.* **76**(1), A57.
68. R. Merkel, E. Sackmann, and E. Evans (1989) *J. Phys. France* **50**, 1535–1555.
69. D. A. Brown and E. London (1997) *Biochem. Biophys. Res. Commun.* **240**, 1–7.
70. D. A. Brown and J. Rose (1992) *Cell* **87**, 507–518.
71. K. Simons and E. Ikonen (1997) *Nature* **387**, 569–572.
72. S. N. Ahmed, D. A. Brown, and E. London (1997) *Biochemistry* **36**, 10944–10953.
73. R. Schroeder, E. London, and D. A. Brown (1994) *Proc. Natl. Acad. Sci. USA* **91**, 12130–12134.
74. D. A. Brown and E. London (1998) *Annu. Rev. Cell Dev. Biol.* **14**, 111–136.
75. S.-L. Lo, and E. L. Chang (1990) *Biochem. Biophys. Res. Commun.* **167**, 238–243.
76. M. De Rosa and A. Gambacorta (1988) *Prog. Lipid Res.* **27**, 153–175.
77. H. Komatsu and P. L.-G. Chong (1998) *Biochemistry* **37**, 107–115.